

Vortex Intersections, Dirac Eigenmodes and Fractional Topological Charge in $SU(2)$ Lattice Gauge Theory

Roman Höllwieser*

Atomic Institute, Vienna University of Technology, Wiedner Hauptstr. 8-10, 1040 Vienna, Austria
E-mail: hroman@kph.tuwien.ac.at

Manfried Faber

Atomic Institute, Vienna University of Technology, Wiedner Hauptstr. 8-10, 1040 Vienna, Austria
E-mail: faber@kph.tuwien.ac.at

Urs M. Heller

American Physical Society, One Research Road, Ridge, NY 11961, USA
E-mail: heller@aps.org

We investigate intersections of thick, plane center vortices, characterized by the topological charge $|Q| = 1/2$, and compare them with the distribution of zeromodes of the Dirac operator in the fundamental and adjoint representation using both the overlap and asqtad staggered fermion formulations in $SU(2)$ lattice gauge theory. We find that Dirac zeromodes do not exactly locate topological charge contributions $|Q| = 1/2$ but are rather sensitive to Polyakov (Wilson) lines.[†]

XXIX International Symposium on Lattice Field Theory
July 10 - 16 2011
Squaw Valley, Lake Tahoe, California

*Speaker.

[†]This research was partially supported by the Austrian Science Fund (FWF) under contract P22270-N16 (R.H.).

1. Introduction

Non-perturbative quantum chromodynamics (QCD) shows quark confinement and spontaneous chiral symmetry breaking (SCSB). Presently, a rigorous treatment of them is only possible in a lattice regularization. Many of the important features of non-abelian gauge theories are already present in $SU(2)$, which simplifies theoretical and numerical calculations. The present numerical investigation concentrates on the topological charge contributions of vortex intersections and their localization by Dirac zeromodes. All measurements were performed on hyper-cubic lattices of even sizes from 12^4 up to 22^4 -lattices. Using the overlap and asqtad staggered Dirac operator, we compute fundamental and adjoint zeromodes in the background of four vortex intersections. By visualizing the probability density, we compare the distribution of the eigenmode density with the position of the vortices and the topological charge density created by intersection points.

2. Plane Vortices

We construct planar vortices with gauge links $U_\mu = \exp(i\phi\sigma_3)$, varying in the σ_3 subgroup of $SU(2)$. For xy -vortices $\mu = t$ links are nontrivial in one t -slice only, for zt -vortices we have nontrivial y -links in one y -slice. Since the $U(1)$ subgroup remains unchanged, the direction of the flux and the orientation of the vortex are determined by the gradient of the angle ϕ , which we choose as a linear function of the coordinate perpendicular to the vortex. Upon traversing a vortex sheet, the angle ϕ increases or decreases by π within a finite thickness $2d$ of the vortex, see Fig. 1a). Center projection leads to a (thin) P-vortex at half the thickness (d) [1]. We consider these thick, planar vortices intersecting orthogonally. As shown in [2], each intersection carries a topological charge with modulus $|Q| = 1/2$, whose sign depends on the relative orientation of the vortex fluxes. We combine xy and zt -vortices in central y - and t -slices with vortex centers at $x_{1,2}$ resp. $z_{1,2}$ located symmetrically around the lattice center and varying vortex thickness d . In Fig. 1b) and Fig. 1c) we present a 3-dimensional view of the intersecting vortices and the topological charge distribution in the (xz) intersection plane.

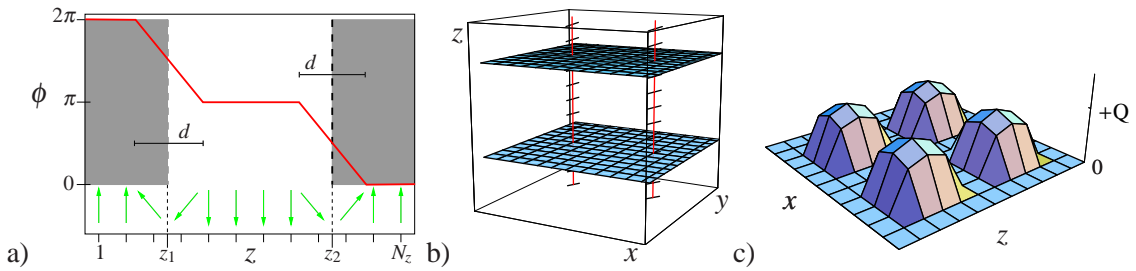


Figure 1: a) The link angle ϕ of a parallel vortex pair. The arrows rotate counterclockwise with increasing ϕ . The vertical dashed lines indicate the positions of the P-vortices. In the shaded areas the links have positive, otherwise negative trace. b) A 3-dimensional section (hyperplane) in xyz -direction of a 12^4 -lattice at time $t = 6$ (center). The horizontal planes are the xy -vortices, which exist only at this time. The vertical lines are the zt -vortices, which continue over the whole time axis. The ticks protruding from the vertical lines extend in time direction. c) The vortices intersect in four points of the $y = t = 6$ - plane, showing four lumps of topological charge $Q = 1/2$, giving total topological charge $Q = 2$.

3. Fermionic zeromodes of the overlap and asqtad staggered Dirac operator for intersecting center vortex fields

We analyze the scalar density $\rho(x) = \psi^\dagger \psi(x)$ of fermionic zeromodes ψ in the background of intersecting plane vortices. As described in [3] the improved staggered operator also produces eigenmodes which can clearly be identified as zeromodes and all results in this paper show perfect agreement between the two fermion realizations. The fermionic zeromodes are used to measure the topological charge Q via the Atiyah-Singer index theorem [4, 5, 6], $\text{ind } D[A] = n_- - n_+ = Q$, where n_- and n_+ are the number of left- and right-handed zeromodes of the Dirac operator D . This equation accounts for Wilson and overlap fermions in the fundamental representation. The adjoint version of the index theorem reads $\text{ind } D[A] = n_- - n_+ = 2NQ = 4Q$, where $N = 2$ is the number of colors and the additional factor 2 is due to the fact that the fermion is in the real representation, hence the spectrum of the adjoint Dirac operator iD is doubly degenerate. The eigenvalues of the staggered fermion operator have a twofold degeneracy due to a global charge conjugation symmetry in $SU(2)$. We therefore have $\text{ind } D[A] = n_- - n_+ = 2Q$ for fundamental and $\text{ind } D[A] = n_- - n_+ = 8Q$ for adjoint (asqtad) staggered fermions.

3.1 Fundamental zeromodes

For the above vortex configuration the four intersection points all carry topological charge contributions of $+1/2$ and therefore sum up to a total topological charge $Q = 2$. In agreement with the lattice index theorem we get two overlap and four asqtad staggered zeromodes of negative chirality (left-handed) in the fundamental representation. Fig. 2 shows the scalar density plots of the fundamental overlap and asqtad staggered zeromodes with periodic boundary conditions together with the sum of Wilson lines in y- and t-direction (Polyakov-loops) in the intersection plane as well as the scalar density plot of the two overlap zeromodes with usual antiperiodic boundary conditions in time direction (asqtad staggered modes again distribute similarly). The individual modes all distribute equally, showing four distinct maxima, as trivially all their linear combinations do. A close look shows that the zeromodes do not exactly peak at the vortex intersections, they rather avoid regions with negative Polyakov lines and approach the intersections (or the vortex surfaces) from regions with positive Polyakov lines. This behavior was already observed in [7] for spherical vortices: the zeromodes avoid regions with negative Polyakov lines.

3.2 Adjoint zeromodes

Adjoint eigenmodes of the Dirac operator are also sensitive to topological charge contributions of $|Q| = 1/2$, but we do not find zeromodes localized to a single vortex intersection. Therefore we use the inverse participation ratio (IPR) [8, 9, 10, 11] to quantify the localization of eigenmodes. The IPR of a normalized ($\sum_x \rho_i(x) = 1$) field $\rho_i(x)$ is defined as $I = N \sum_{x=0}^N \rho_i^2(x)$, where N is the number of lattice sites x . With this definition, I characterizes the inverse fraction of sites contributing significantly to the support of $\rho(x)$, *i.e.*, a high IPR indicates that the eigenmode is localized to a few lattice points only. We perform systematic and random IPR maximization procedures for linear combinations of zeromodes in order to get single eigenmode peaks localized to regions with nonvanishing topological charge contribution. Our vortex configuration gives 8 overlap and 16 asqtad staggered adjoint Dirac zeromodes with negative chirality for antiperiodic

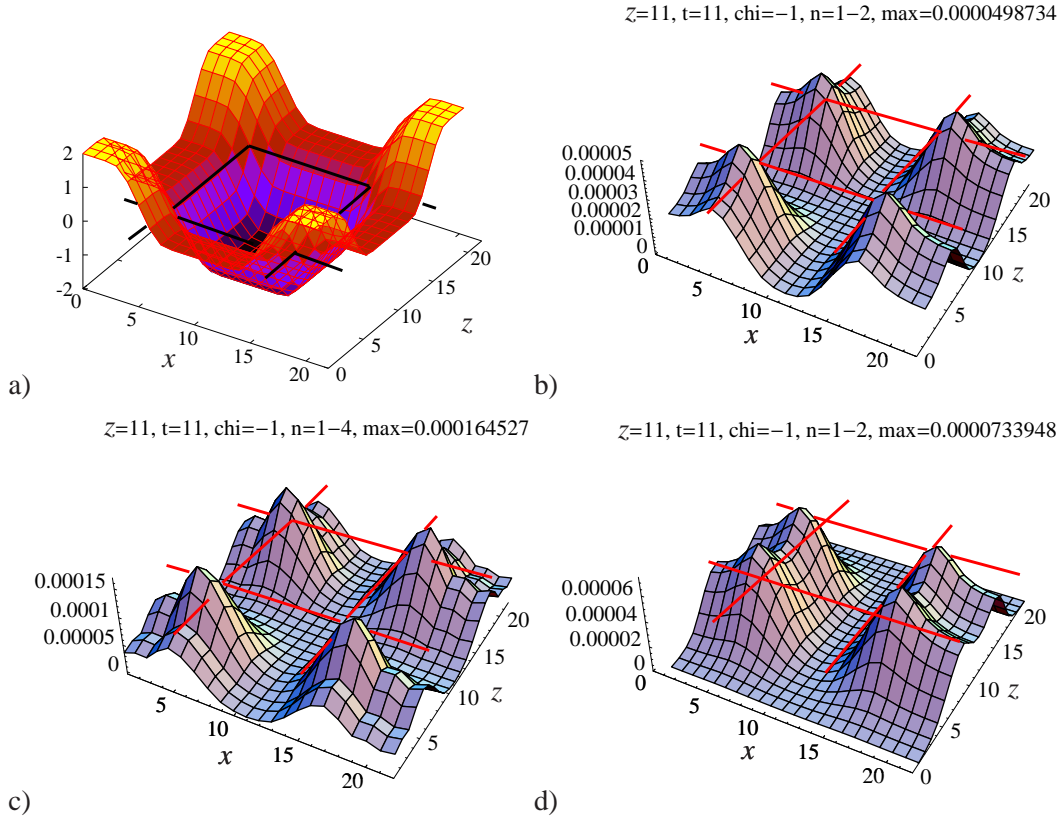


Figure 2: a) Sum of Wilson lines in y - and t -direction (Polyakov-loops) in the intersection plane. P-vortices are indicated with black lines. Scalar density plots of b) the two overlap zero modes, c) the four asqtad staggered zero modes, both with periodic boundary conditions, and d) the two overlap zero modes with anti-periodic boundary conditions in time direction. The plot titles indicate the plane positions, the chirality ($\text{chi}=\pm 1$) and numbers ($n=1-2/n=1-4$) of (overlap/asqtad staggered) zero modes and the maximum density peak in the plot. P-vortices are indicated with red lines.

boundary conditions in time direction. Fig. 3 shows their scalar densities, they locate the xy -vortex pairs but even individual modes do not show single peaks locating one intersection with $Q = 1/2$. Linear combinations of the eight overlap zero modes with negative chirality show six distinct IPR maxima. This was obtained by a systematic study with the eight coefficients of the linear combination varying from -10 to 10 in integer steps. Further we started from 20.000 random points in the parameter space and determined the nearest maximum by the gradient method. Each of the six maxima was found between 2.000 – 6.000 times and no other maxima were obtained. In Fig. 3e we plot a 2D cut through the first three IPR maxima in the 8D parameter space of linear combinations. The scalar density of the linear combination of the eight zero modes with maximal IPR is presented in Fig. 3d, it still peaks at two vortex intersections. Therefore, we analyze a configuration of "thin-thick" vortex intersections apparently having topological charge $|Q| = 1/2$. The profile of a "thin-thick" vortex is plotted in Fig. 4a. The thin vortex sheet is defined by the jump of the y - or t -link from $+1$ to -1 at the boundary. The thick vortex is located symmetrically around the center of the lattice with thickness d . The thin-thick xy - and zt -vortices still intersect at

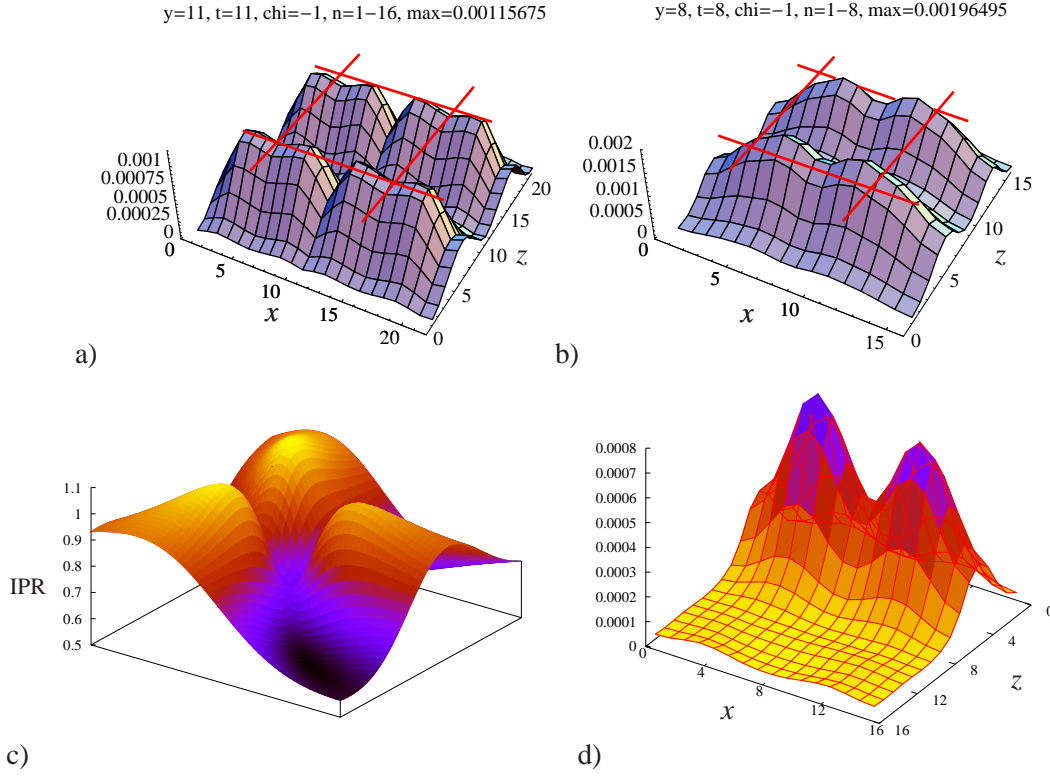


Figure 3: Scalar density plots of the a) 16 asqtad staggered and b) eight overlap left-handed adjoint zero modes for antiperiodic boundary conditions, the modes locate the xy -vortex pair. c) Plane through the highest three IPR maxima in the parameter space of linear combinations of the eight zero modes. The peaks are very broad and easy to identify. d) The scalar density of the linear combination of the eight zero modes with maximal IPR still peaks at two vortex intersections.

four points, but the plaquette or hypercube definitions of topological charge do not recognize the thin vortex sheets and only measure one topological charge contribution $Q = 1/2$ of the "thick" vortex intersection, see Fig. 4b. We use antiperiodic boundary conditions in time direction and get no fundamental zero modes for this " $|Q| = 1/2$ configuration". The adjoint Dirac operator gives two adjoint overlap and four adjoint staggered zero modes with negative chirality, which due to the index theorem again result in $Q = 1/2$. For the adjoint fermions this configuration truncates three of the four vortex intersections and in this way simulates a situation related to the one achieved by twisted boundary conditions, namely, a single detectable intersection. Therefore it is possible to have a configuration that looks like having fractional topological charge. The eigenmode density distributions of overlap and asqtad staggered zero modes are identical. Fig. 5 shows the former for the intersection plane and for planes orthogonal to it at the (thick) intersection point. The modes are clearly sensitive to the traces of the adjoint links U_A (see also Fig. 4a), defined by $(\text{Tr}U)(\text{Tr}U)^\dagger = (\text{Tr}U)^2 = 1 + \text{Tr}U_A$, which in our configuration define the adjoint Polyakov lines P_A (Wilson lines). The zero modes prefer regions of positive Polyakov lines and avoid negative Polyakov lines. Due to the antiperiodic boundary conditions in time direction the signs of the Polyakov lines are exchanged. Hence, the zero mode densities peak at the xy -vortex center and avoid the zt -vortex center, or rather peak at the boundary parallel to the zt -vortex.

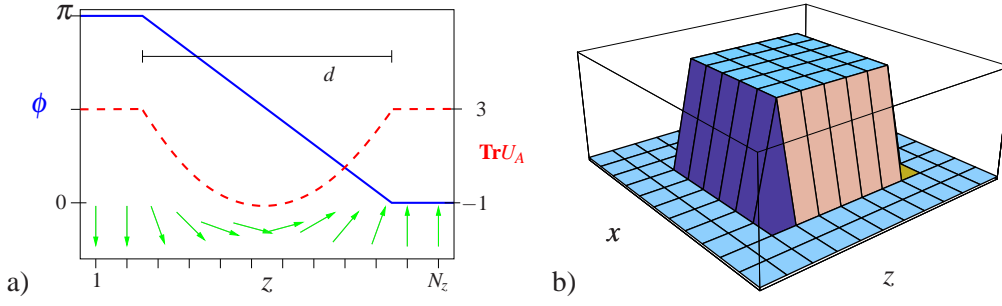


Figure 4: a) Link profile of a "thin-thick" plane vortex, the link angle ϕ (blue) decreases from π to 0 within a certain vortex thickness d . The thin vortex is given by the jump at the boundary. The red dashed line shows the trace of adjoint links $\text{Tr}U_A$ (see text below) b) Topological charge density in the intersection plane.

4. Conclusions

The zeromodes of the asqtad staggered and overlap Dirac operators in the background of intersecting vortex configurations are shown to be sensitive to the value of the Polyakov loops (Wilson lines), avoiding regions with negative Polyakov loops. With adjoint fermions we tried to find zeromodes which identify exactly one topological charge contribution $Q = 1/2$ of a single vortex intersection. Therefore, we analyzed linear combinations of zeromodes which maximize the inverse participation ratio (IPR), *i.e.*, localize as much as possible. We found that the scalar eigenmode density of adjoint fermions always peaks at least at two intersections. Further, we analyzed a lattice configuration with only one "thick" vortex intersection. Since both, gluonic and (adjoint) fermionic definitions of topological charge fail to detect intersections with at least one thin vortex, both definitions of Q merely signal the value $Q = 1/2$. It is remarkable, that for this case of only one detectable vortex intersection, the adjoint zeromodes spread over the whole lattice, avoiding regions of negative traces of adjoint Polyakov (Wilson) lines. They are not localized to the region with nonvanishing topological charge contribution. Thus, we conclude that the Dirac zeromodes are more sensitive to the Polyakov (Wilson) lines than to the topological charge contributions for the configurations considered in this work.

References

- [1] Del Debbio, L. and Faber, M. and Greensite, J. and Olejník, Š. Center dominance and $Z(2)$ vortices in $SU(2)$ lattice gauge theory. *Phys. Rev.*, D55:2298–2306, 1997.
- [2] M. Engelhardt and H. Reinhardt. Center projection vortices in continuum Yang-Mills theory. *Nucl. Phys.*, B567:249, 2000.
- [3] Höllwieser, Roman and Faber, Manfred and Heller, Urs M. Lattice Index Theorem and Fractional Topological Charge. [arXiv:hep-lat/1005.1015], 2010.
- [4] M. F. Atiyah and I. M. Singer. The Index of elliptic operators. 5. *Annals Math.*, 93:139–149, 1971.
- [5] A. S. Schwarz. On Regular Solutions of Euclidean Yang-Mills Equations. *Phys. Lett.*, B67:172–174, 1977.
- [6] Lowell S. Brown, Robert D. Carlitz, and Choon-kyu Lee. Massless Excitations in Instanton Fields. *Phys. Rev.*, D16:417–422, 1977.

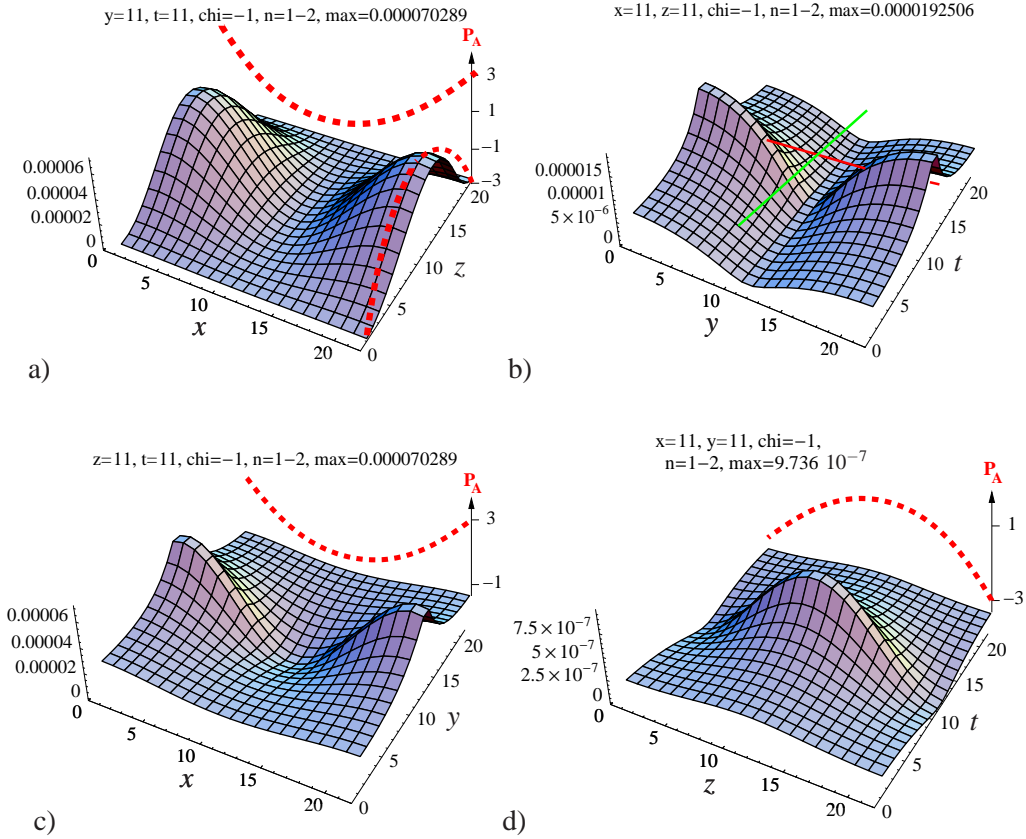


Figure 5: Scalar eigenmode density of the two left-handed adjoint overlap (identical to four adjoint asqtad staggered) zeromodes in various planes through the thick-thick vortex intersection: a) xz -plane (intersection plane): The zeromodes avoid regions of negative adjoint Polyakov (Wilson) lines (P_A , red dots) with respect to boundary conditions and therefore do not peak at the topological charge contribution $Q = 1/2$; b) yt -plane: The antiperiodic boundary conditions invert the profile in time- compared to the one in y -direction, hence the zeromodes prefer the xy -vortex (red) and avoid the zt -vortex (green); c) xy -plane: The zeromodes reflect the profile of the adjoint y -Wilson lines of the zt -vortex in x -direction; d) zt -plane: The zeromodes reflect the profile of the adjoint Polyakov lines of the xy -vortex in z -direction, inverted by the antiperiodic boundary conditions in time direction.

- [7] Jordan, Gerald and Höllwieser, Roman and Faber, Manfred and Heller, Urs M. Tests of the lattice index theorem. *Phys. Rev.*, D77:014515, 2008.
- [8] E. M. Ilgenfritz et al. Exploring the structure of the quenched QCD vacuum with overlap fermions. *Phys. Rev.*, D76:034506, 2007.
- [9] M. I. Polikarpov, F. V. Gubarev, S. M. Morozov, and V. I. Zakharov. Localization of low lying eigenmodes for chirally symmetric Dirac operator. *PoS*, LAT2005:143, 2006.
- [10] C. Aubin et al. The scaling dimension of low lying Dirac eigenmodes and of the topological charge density. *Nucl. Phys. Proc. Suppl.*, 140:626–628, 2005.
- [11] C. Bernard et al. More evidence of localization in the low-lying Dirac spectrum. *PoS*, LAT2005:299, 2006.